SPECTRA OF VARIOUS HADRONS AND THEIR FREEZE-OUT PARAMETERS AT DIFFERENT CENTRALITIES AT THE RHIC ENERGY OF $\sqrt{s_{NN}} = 200$ GeV

Riyaz Ahmed Bhat

Research Lab., Govt. Degree College (Boys) Anantnag, J&K, India
riyaztheory@gmail.com

Saeed Uddin

Department of Physics, Jamia Millia Islamia, New Delhi-110025, India

(Received October 2, 2017; accepted November 29, 2017)

The transverse momentum spectra of various hadrons at different centralities at the RHIC energy of $\sqrt{s_{NN}} = 200$ GeV are studied. The study is based on a unified statistical thermal freeze-out model which incorporates the longitudinal as well as transverse boosts. The model also incorporates the dependence of the baryonic chemical potential on rapidity of the forward fireballs distributed along the longitudinal axis. The transverse momentum spectra have been found to be in close agreement with the available RHIC experimental data at all centralities. The kinetic freeze-out parameters are extracted by comparing our model results with the experimental data using the method of minimization of χ^2/DOF. The extracted parameters indicate that the freeze-out temperature increases with decreasing centrality, while the collective flow velocity increases with the increase in centrality of the colliding system. The work is studied with the inclusion of all heavier resonance decay contributions.

DOI:10.5506/APhysPolB.49.15

1. Introduction

The experimental study of nuclear matter at extreme temperatures and densities offers a unique opportunity for insight into the properties of strongly interacting many-body systems, as described by non-perturbative quantum chromodynamics (QCD). One important aspect of these studies is the search for the predicted phase transition to a color-deconfined state of quarks and gluons of such a system called Quark–Gluon Plasma. In nature, such systems exist only in astrophysical objects, like neutron stars and collapsing supernovae. In the laboratory, long-range properties of nuclear matter can be studied only by means of heavy-ion collisions for comparatively small systems and short times. By varying the bombarding energy as well as projectile and target combinations, it is possible to create systems of different energy and baryon density. This allows the study of new phases of nuclear matter. At low densities, a phase transition from the nuclear liquid to a gas of nucleons is investigated, whereas at high densities ($n_{\rm B} = 0.72/{\rm fm}^3$), about five times normal nuclear matter density, the phase transition to the quark–gluon plasma is predicted to occur, where chiral symmetry is restored and quarks are deconfined. Lattice simulations have shown that the transition is a crossover for $\mu_{\rm B} = 0$ MeV [1]. The benchmark value of energy density is $\epsilon = 1~{\rm GeV/fm}^3 = 1.8\times10^{15}{\rm g~cm}^{-3}$. The corresponding relativistic matter pressure is $P \approx \frac{1}{3}\epsilon = 0.52\times10^{30}$ bar. This dense matter must have existed in the early universe just about 10 μs after the Big-Bang. This is difficult to model analytically — description in terms of the hadronic degrees of freedom breaks down as one approaches the crossover temperature. Recent terminology for the QCD state near the crossover $T \sim (1-2)\,T_{\rm C}$ is strongly coupled quark–gluon plasma (sQGP) [2].

Identifying and studying the properties of these phases is a challenging task that requires knowledge of the evolution of the hadronic phase and its macroscopic properties. Experimental phenomenology provides valuable input to theory, which at present is not able to model the complete dynamics of a heavy-ion collision because of the non-perturbative nature of the processes involved.

Within the framework of the statistical model, it is assumed that a hot fireball, formed during collisions of relativistic nuclei, undergoes expansion accompanied by a decrease in its temperature. If the initial temperature of a fireball $T_{\rm i}$ is high, then it is in a quark–gluon plasma (QGP) state. At the transition temperature $T_{\rm c}$, quarks and gluons form hadrons and the system is in the mixed state. When the temperature $T < T_{\rm c}$, a hadronic gas expands further ending up in a system decaying into non-interacting secondary hadrons. This process is called fireball freeze-out and it starts the moment at which the rate of microscopic hadronic interactions becomes comparable to that of macroscopic expansion of a system. The constituents of the hot and dense medium produced during a heavy-ion collision interact with each other by inelastic and elastic collisions and it evolves into a state of free particles. This process of hadronic decoupling is called freeze-out. Two kinds of freeze-out are found: chemical freeze-out ($T_{\rm f}^{\rm ch}$) when inelastic collisions cease and the particle yields (ratios) become fixed; thermal (kinetic) freeze-out $T_{\rm f}^{\rm th}$ when elastic collisions cease and particle transverse momenta spectra get fixed. The estimation of the macroscopic properties of the chemical freeze-out can be extracted from particle ratios. These parameters collected over the last two decades seem to follow regular patterns as the beam energy increases [3–5]. The higher moments have been suggested to control the freeze-out, so the several conditions has been proposed [6]. The fluctuations of the conserved quantities are done on the basis of HRG model and the comparison is made on the moments of the multiplicity distribution of specific particles to the experimental data to extract T and μ_{B} [7, 8]. The study of higher moments of various conserved quantities such as baryon number, strangeness and charge would indicate a critical behaviour in the QCD phase diagram [9]. The important or the crucial question is whether at the time of hadronisation, the thermal system generated in these collisions has kept memory of the plasma phase or the expansion period during which it may have passed by a critical point. This memory should reflect in higher moments of charge distributions [10].

It is believed that the produced hadrons carry information about the collision dynamics and the subsequent space-time evolution of the system. Hence, a precise measurement of the transverse momentum (p_{T}) distribution of identified hadrons is essential for the understanding of the dynamics and properties of the created matter up to the final hydro-dynamic freeze-out. The measurements of particle abundances and transverse momentum distributions could provide information about the final stages of the evolution at chemical and kinetic freeze-out. Hydrodynamical models [11–13] that include radial flow successfully describe the measured p_{T} distributions in Au+Au collisions at $\sqrt{s_{NN}} = 130$ GeV [14, 15]. The p_{T} spectra of identified charged hadrons below 2 GeV/c in central collisions have been well-reproduced in some models by two simple parameters: transverse flow velocity β_{T} and thermal freeze-out temperature T under the assumption of thermalization. Some statistical models have successfully described the particle abundances at low p_{T} [16–18].

We present a study of transverse momentum distribution of hadrons coming from hadronic fluid elements *versus* centrality using a thermal freeze-out model which incorporates both the longitudinal and transverse boosts. The results are presented for mid-rapidity region.

We also present a study of the centrality dependence of thermal freeze-out temperature and collective flow velocity at the hydro-thermal freeze-out in Au+Au collisions at mid-rapidity for the RHIC energy of $\sqrt{s_{NN}} =$ 200 GeV. The term collectivity denotes a common feature that is observed for several particles emerging from one reaction. Collective flow is the prototype of such a common feature and describes a movement of a large number of ejectiles either in a common direction or at a common magnitude of velocities.

2. The model

The momentum distributions of hadrons, emitted from within an expanding hadronic fireball in the state of local thermal equilibrium, are characterized by the Lorentz-invariant Cooper–Frye formula [11]

$$E\frac{\mathrm{d}^3 n}{\mathrm{d}^3 p} = \frac{g}{(2\pi)^3}\int\limits_{\Sigma_\mathrm{f}} f\left(\frac{p^\mu u_\mu}{T},\lambda\right) p^\mu \mathrm{d}\Sigma_\mu\,, \tag{1}$$

where g is the degeneracy factor, λ is the fugacity factor, Σ_f is the hyper freeze-out surface and the function f is a quantum distribution function. In our study, our 'matter' of interest consists of individually confined hadronic particles. At sufficiently high temperature, a high density of hadronic particles can arise as a consequence of many hadron species contributing, and does not, in general, imply a quantum degeneracy of the phase space or, in other words, in a very rich multicomponent phase, each particle species has a rather low 'non-degenerate' phase space abundance and, therefore, we employ here the classical (Boltzmann)-gas limit.

In order to obtain the particle spectra in the overall rest frame of the hadronic fireball, we first define the invariant cross section for a given hadron in the local rest frame of the expanding hadronic fluid element. As the invariant cross section will have the same value in all Lorentz frames, we can thus write

$$E\frac{\mathrm{d}^3 n}{\mathrm{d}^3 p} = E'\frac{\mathrm{d}^3 n}{\mathrm{d}^3 p'}\,. \tag{2}$$

The unprimed quantities on the LHS of above equation refer to the invariant spectra of a given hadronic species in the overall rest frame of hadronic fireball formed in the ultra-relativistic nuclear collisions, and the primed quantities on the RHS refer to the invariant spectra of the same hadronic species but in the rest frame of a local hadronic fluid element.

The distribution function is given as

$$\frac{\mathrm{d}^3\, n}{\mathrm{d}^3\, p} \sim \frac{1}{\exp\left[\left(E-\mu_\mathrm{B}\right)/T\right] \pm 1}\,, \tag{3}$$

where $+$ sign and $-$ sign are for fermions and bosons, respectively, and μ_B is the baryonic chemical potential.

In recent works, it has been clearly shown that there is strong evidence of increasing baryon chemical potential, μ_B, along the collision axis in the RHIC experiments. We can parametrize the baryonic chemical potential as a function of expanding fireball rapidity as [19, 20]

$$\mu_\mathrm{B} = a + b\, y_0^2\,, \tag{4}$$

where the constants a and b are fitting parameters (in units of MeV) and determine the degree of transparency/stopping in a heavy-ion collision. The quadratic-type dependence of the baryonic chemical potential, $\mu_{\rm B}$ on y_0 has been also considered in the above equation so as to make $\mu_{\rm B}$ invariant under the transformation $y_0 \to -y_0$, as the system properties are to remain invariant under the above transformation.

Furthermore, the energy and momentum of the particle in the local hadronic fluid element frame (primed) in terms of the unprimed quantities are given by the Lorentz transformation as

$$E' = \gamma \left(E - \vec{p} \cdot \vec{\beta} \right) \qquad \text{with} \qquad \vec{p} \cdot \vec{\beta} = p_{\rm T}\beta_{\rm T} + p_z\beta_z \tag{5}$$

and $p' = \sqrt{E'^2 - m^2}$, where $p_{\rm T}$ and p_z are, respectively, the transverse and longitudinal momentum of the particle in the overall rest frame of the hadronic fireball. Similarly $\beta_{\rm T}$ and β_z are, respectively, the transverse and longitudinal components of the expansion velocity (β) of a hadronic fluid element and γ is the Lorentz factor. We assume that the expanding hadronic fluid element does not have any amount of whirl velocity component (*i.e.* azimuthal component) hence we have $\beta_\phi = 0$.

The energy and longitudinal momentum of the particle in terms of rapidity and transverse mass are given as

$$E = m_{\rm T} \cosh y \,, \qquad p_z = m_{\rm T} \sinh y \,. \tag{6}$$

Since the fireball has the longitudinal as well as the transverse expansion velocity components, the transverse velocity component of the hadronic fireball is assumed to vary with the transverse coordinate r as [21]

$$\beta_{\rm T}(r) = \beta_{\rm T}^{\rm s} \left(\frac{r}{R} \right)^n \,, \tag{7}$$

where n is the index of the profile, R is the size of the fireball and is equal to r_0 at mid-rapidity, and $\beta_{\rm T}^{\rm s}$ is the surface transverse expansion velocity and is fixed in the model by using the following parameterization:

$$\beta_{\rm T}^{\rm s} = \beta_{\rm T}^{0} \sqrt{1 - \beta_z^2} \,. \tag{8}$$

Taking the spatial z-coordinate dependence of the forward fireball rapidity, a simple kinematics yield the following expression for the longitudinal velocity component of the hadronic fluid element:

$$\beta_z(z) = \tanh(cz) \,. \tag{9}$$

In the above equation when $z \to 0$, we obtain $\beta_z(z) \to 0$, while for $z \to \infty$, we obtain $\beta_z(z) \to 1$. This variable *i.e.*, z is an integration variable in our model to get the contribution towards the yield of any particle specie from all the fireballs distributed along the collision axis.

The above relation is also required to ensure that the velocity β of any fluid element must satisfy

$$\beta = \sqrt{\beta_{\mathrm{T}}^2 + \beta_z^2} \leq 1\,. \tag{10}$$

In our analysis, we have used $c = 1$ as it provides a good fit to the overall data. We also parameterize R as [21]

$$R = r_0 \exp\left(-\frac{z^2}{\sigma^2}\right)\,, \tag{11}$$

where r_0 is the model parameter which fixes the transverse size of the hadronic matter and σ is the width of the distribution.

A first analysis of the data obtained by the BRAHMS Collaboration at $\sqrt{s_{NN}} = 200$ GeV was done by Stiles and Murray [19]. This shows a strong evidence of the dependence of baryon chemical potential on rapidity due to the changing nature of $\bar{P}/P$ ratio with rapidity. The general procedure of our model is as follows: the rapidity axis or the collision axis is populated with the hot hadronic fluid elements with increasing chemical potentials with the co-ordinate of the collision axis (z-axis). Unlike earlier assumption of the temperature to be also rapidity-dependent, it is assumed to be the same for all the hadronic fluid elements. At the final *hydrodynamic freeze-out*, which follows the thermo-chemical freeze-out, the emitted particles leave the different regions of the fireball following a local (thermal) distribution. The resulting rapidity distribution or transverse momentum distribution of any given particle specie is then obtained by a superposition of the contribution of these regions.

3. Results

In the earlier analysis [20], the width of the distribution, that is σ, was determined from π^+ distribution as these are very sensitive to the value of sigma and less to the variation of baryon chemical potential. In our study, the width of the distribution is chosen as a fit parameter and is taken to be 4.30 for the best fit of all the spectra. The model parameters a and b have an insignificant effect on the transverse momentum distribution of particles and, therefore, are fixed to be 22.4 MeV and 9.1 MeV, respectively, as these values exactly fit the rapidity distribution of all the particle species at $\sqrt{s_{NN}} = 200$ GeV [22]. These parameters are more important in dealing with the nuclear stopping/transparency. Stopping is a measure of efficiency of converting the incoming longitudinal energy of a projectile and target into transverse degrees of freedom, hence slowing down the motion of incoming nucleons. The signatures of incomplete stopping and of a longitudinally expanding source lead to similar rapidity distributions of the emitted particles.

The shape of the collective flow velocity profile has also some effect on the spectra because of the non-linearity in the dependence of the spectral shape on the flow velocity. Therefore, the value of n is fixed to be unity.

The transverse momentum distribution for protons and anti-protons at different centralities is shown in figure 1. The T_{kin} decreases from peripheral to central collisions. The collective expansion velocity increases with the increase in centrality. The profile of the thermal freeze-out conditions for proton and anti-proton at different centralities along with the χ^2/DOF for each fit is shown in Table I. The error in the thermal freeze-out temperature and collective flow velocity at all centralities for the hadrons studied are, respectively, in the domain of $-0.005 < \mathrm{error}\,(\beta_{\mathrm{T}}) < 0.005$ and $-0.5 < \mathrm{error}\,(T) < 0.5$. The extracted parameters correspond to the scenario where chemical and kinetic freeze-out is considered to take place simultaneously. Such single freeze-out scenarios have been discussed in Ref. [12, 23]. It is clear from Table I that the collective flow motion decreases from central to peripheral collisions. Also proton and anti-proton have almost the simultaneous freeze-out at all centralities.

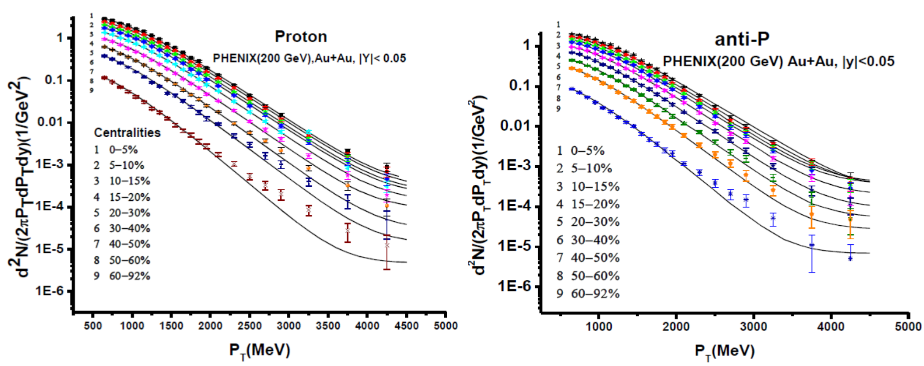

Fig. 1. Transverse momentum distribution of protons (left panel) and anti-protons (right panel) at different centralities (PHENIX Collaboration) for Au + Au colliding system at $\sqrt{s_{NN}} = 200$ GeV.

The particles at the surface of the hot and dense zone are likely to decouple earlier, while the particles inside the hot zone collide with each other and hence try to attain a net collective velocity. This is because the probabilities of the collision towards the inside and the outside are different. This makes the motion of the particles less random. This effect is more prominent in central collisions and shows least effect in peripheral collisions. The freeze-

TABLE I

Freeze-out parameters at different centralities and their respective χ^2/DOF obtained from the best fit of proton and anti-proton p_{T}-distribution (PHENIX data). The errors associated with the values of T and β_{T} are, repectively, in the domains $< |0.5|$ and $< |0.005|$.

Centrality	$(T$ [MeV], $\beta_{\mathrm{T}}^0)$ Proton	χ^2/DOF	$(T$ [MeV], $\beta_{\mathrm{T}}^0)$ anti-Proton	χ^2/DOF
(0–5)%	(162, 0.66)	0.88	(163, 0.67)	2.97
(5–10)%	(163, 0.66)	0.88	(163, 0.67)	2.97
(10–15)%	(164, 0.65)	0.44	(164, 0.65)	1.28
(15–20)%	(164, 0.65)	0.53	(164, 0.66)	1.21
(20–30)%	(166, 0.63)	0.53	(167, 0.63)	0.92
(30–40)%	(168, 0.60)	1.28	(168, 0.60)	0.26
(40–50)%	(169, 0.56)	1.42	(168, 0.57)	0.63
(50–60)%	(172, 0.51)	1.54	(170, 0.51)	0.70
(60–92)%	(174, 0.40)	2.33	(171, 0.42)	1.35

out temperature corresponding to more heavier particles such as cascades and omegas are even higher but does not show higher collective flow velocity. The centrality dependence of the transverse momentum distribution of Λ and $\bar{\Lambda}$ is shown in figure 2. The profiles of the thermal freeze-out conditions with the centrality for Λ and $\bar{\Lambda}$ are shown in Table II. The minimum χ^2/DOF for the most central collisions for the distributions of P, $\bar{P}$, Λ and $\bar{\Lambda}$ are given, respectively, as 0.88, 2.97, 1.31 and 1.84.

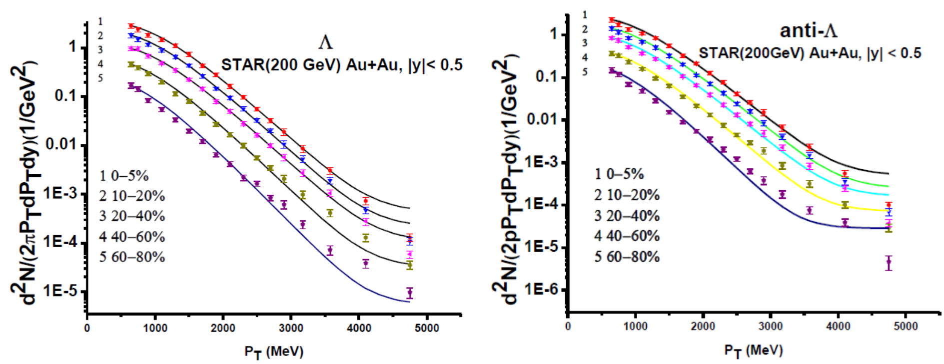

Fig. 2. Transverse momentum distribution of Λ (left panel) and $\bar{\Lambda}$ (right panel) at different centralities (STAR Collaboration) for Au + Au colliding system at $\sqrt{s_{NN}} = 200$ GeV.

TABLE II

Freeze-out parameters at different centralities and their respective χ^2/DOF obtained from the best fit of Lambda and anti-Lambda p_{T}-distribution (STAR data). The errors associated with the values of T and β_{T} are, respectively, in the domains $< |0.5|$ and $< |0.005|$.

Centrality	$(T$ [MeV], $\beta_{\mathrm{T}}^0)$ Lambda	χ^2/DOF	$(T$ [MeV], $\beta_{\mathrm{T}}^0)$ anti-Lambda	χ^2/DOF
(0–5)%	(167, 0.60)	1.31	(167, 0.60)	1.84
(10–20)%	(169, 0.59)	0.96	(169, 0.59)	1.50
(20–40)%	(171, 0.59)	0.87	(171, 0.57)	1.47
(40–60)%	(172, 0.53)	1.46	(174, 0.52)	2.13
(60–80)%	(172, 0.45)	5.83	(176, 0.41)	5.03

The values of the extracted freeze-out temperature obtained for these hadrons is larger than the QCD phase transition temperature obtained from Lattice QCD calculations [24]. One possible reason of higher temperature could be that the transition of quarks and gluons into hadrons drives the equilibration and hence the chemical freeze-out may lie close to the transition temperature, T_{c}. Further, we are trying to modify/incorporate more realistic assumptions/findings in our model so that the value of the thermal freeze-out parameters will be lowered compared to the stated values in Tables I, II and III. A very crude approximation being that the size of the fireball is assumed to be constant during the freeze-out scenario of all the particles (a static fireball approximation). Also the decay products from hadronic resonances are assumed to be in equilibrium with the primary thermal equilibrium which, in other words, do not get enough time to re-scatter from surrounding matter, thus the non-thermal equilibrium is combined with the primary thermal equilibrium to form the final spectrum.

The beauty of the model is that a single function is used to fit the whole range of p_{T} distribution of p_{T} values from 650 MeV to 4250 MeV (22 data points) of a given hadron (*e.g.*, proton and anti-proton) with a single set of model parameters.

However, the values of the extracted temperature could substantially change for meson p_{T} distribution which will be investigated in a future work. The centrality dependence of the transverse momentum distribution of Ξ^+ and Ξ^- is shown in figure 3. The profile of the freeze-out conditions for Ξ^+ and Ξ^- is shown in Table III. The minimum χ^2/DOF for most central collisions for the distributions of these particles are, respectively, obtained as 0.40 and 0.72.

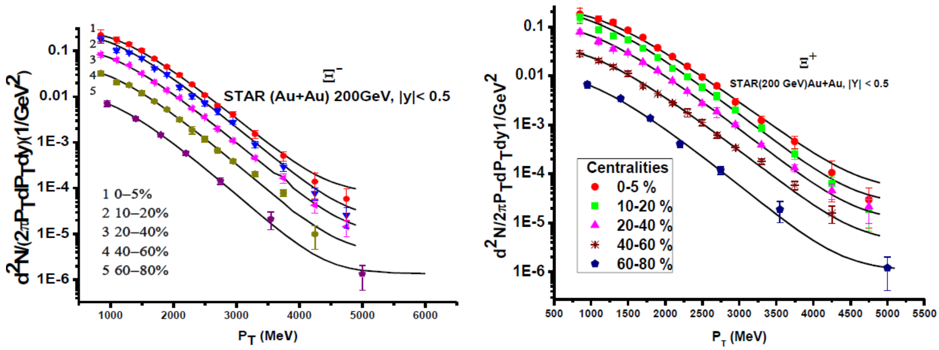

Fig. 3. Transverse momentum distribution of Ξ (left panel) and $\bar{\Xi}$ (right panel) at different centralities (STAR Collaboration) for Au + Au colliding system at $\sqrt{s_{NN}} = 200$ GeV.

TABLE III

Thermal freeze-out parameters for Ξ^+ and Ξ^- at different centralities. The errors associated with the values of T and β_{T} are, respectively, in the domains $< |0.5|$ and $< |0.005|$.

Centrality	$(T$ [MeV], $\beta^0_{\mathrm{T}})$ Cascade	$(T$ [MeV], $\beta^0_{\mathrm{T}})$ anti-Cascade
(0–5)%	(183, 0.60)	(183, 0.61)
(10–20)%	(185, 0.55)	(185, 0.54)
(20–40)%	(190, 0.55)	(189, 0.54)
(40–60)%	(190, 0.53)	(190, 0.54)
(60–80)%	(197, 0.47)	(200, 0.46)

The singly and doubly strange particles show a somewhat higher temperature and lower collective flow velocity than those of non-strange particles. The increase in temperature for strange particles is due to their early freeze-out and hence show low collective or hydrodynamical effects which are not present during the initial stages of the collision. These hydrodynamical effects develop in the later stages of the collision due to large number of collisions and a drop in temperature of the fireball.

The transverse momentum distribution of $\Omega^+ + \Omega^-$ is fitted with the collective flow velocity of 0.33 and a kinetic/thermal freeze-out temperature of 208 MeV. The transverse momentum distribution of $\Omega^+ + \Omega^-$ is shown in figure 4. The minimum χ^2/DOF for the distribution is 2.1.

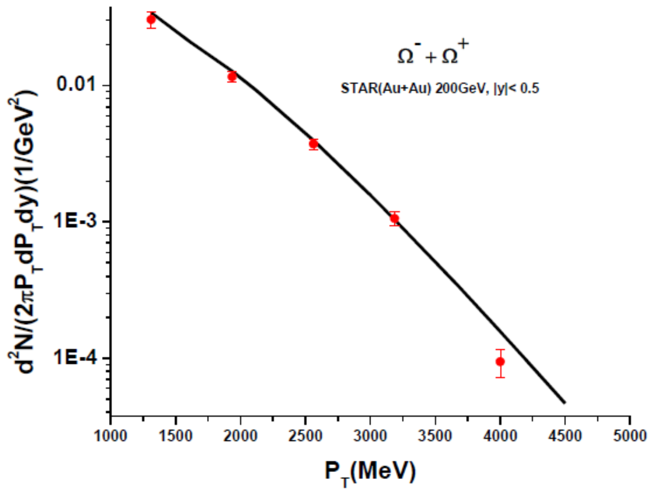

Fig. 4. Transverse momentum distribution of $\Omega^{+} + \Omega^{-}$ for 0–20 % centrality for Au + Au colliding system at $\sqrt{s_{NN}} = 200$ GeV.

4. Summary and conclusion

The sequential freeze-out of various hadrons is studied by using a unified statistical thermal freeze-out model with simultaneous chemical and kinetic freeze-out. The transverse momentum distribution of P, $\bar{P}$, Λ, $\bar{\Lambda}$, Ξ, $\bar{\Xi}$ and $(\Omega^{+} + \Omega^{-})$ are shown to fit well with the RHIC experimental data for Au + Au collision for different centrality bins at $\sqrt{s_{NN}} = 200$ GeV. Kinetic freeze-out parameters are obtained by fitting the experimental data available with our model results using minimum χ^2/DOF method. For the beam energy studied, the central collisions are characterized by a lower T_{kin} and larger β_{T}^{0}, while the peripheral collisions are found to have a higher T_{kin} and smaller β_{T}^{0}. It is also clear that the heavier particles correspond to higher thermal freeze-out temperature as compared to lighter particles. This is because of their early thermo-chemical freeze-out from the hadronic fluid element. Further, the values of the thermal freeze-out temperature extracted for these hadrons are found to be larger than the transition temperature obtained from Lattice QCD calculations. These values of freeze-out parameters could substantially change for the distribution of mesons which will be investigated in a future work.

R.A. Bhat is grateful to the Science and Engineering Research Board (SERB), New Delhi for providing financial support through the project Young Scientist Award.

REFERENCES

[1] K. Szabo, *PoS* **LAT2006**, 149 (2006).

[2] M. Stephanov, *PoS* **LAT2006**, 024 (2006) [`arXiv:hep-lat/0701002v2`].

[3] A. Tawfik, *Adv. High Energy Phys.* **574871**, (2013).

[4] J. Cleyman, H. Oeschler, K. Redlich, S. Wheaton, *Phys. Rev. C* **73**, 034905 (2006).

[5] A. Tawfik, *Nucl. Phys. A* **764**, 387 (2006).

[6] F. Karsch, *J. Phys. G* **38**, 124098 (2011).

[7] V. Mantovani Sarti *et al.*, *Web. Conf.* **97**, 00019 (2015).

[8] Jing-Hua Fu, *Phys. Rev. C* **96**, 034905 (2017) [`arXiv:1610.07138 [nucl-th]`].

[9] J. Thäder, *Nucl. Phys. A* **956**, 320 (2016).

[10] F. Karsch, K. Redlich, *Phys. Lett. B* **695**, 136 (2011) [`arXiv:1007.2581v1 [hep-ph]`].

[11] F. Cooper, G. Frye, *Phys. Rev. D* **10**, 186 (1974).

[12] W. Broniowski, W. Florkowski, *Phys. Rev. Lett.* **87**, 272302 (2001); *Phys. Rev. C* **65**, 064905 (2002).

[13] D. Teaney, J. Lauret, E.V. Shuryak, *Phys. Rev. Lett.* **86**, 4783 (2001).

[14] K. Adcox *et al.* [PHENIX Collaboration], *Phys. Rev. Lett.* **88**, 242301 (2002).

[15] C. Adler *et al.* [STAR Collaboration], *Phys. Rev. Lett.* **87**, 262302 (2001).

[16] F. Becattini *et al.*, *Phys. Rev. C* **64**, 024901 (2001).

[17] P. Braun-Munzinger, D. Magestro, K. Redlich, J. Stachel, *Phys. Lett. B* **518**, 41 (2001).

[18] W. Florkowski, W. Broniowski, M. Michalec, *Acta Phys. Pol. B* **33**, 761 (2002).

[19] L.A. Stiles, M. Murray, `arXiv:nucl-ex/0601039`.

[20] F. Becattini, J. Cleyman, J. Strumpfer, *PoS* **CPOD07**, 012 (2007) [`arXiv:0709.2599 [hep-ph]`].

[21] R.A. Bhat, S. Uddin, I.-ul Bashir, *Nucl. Phys. A* **935**, 43 (2015).

[22] S. Uddin *et al.*, *Nucl. Phys. A* **934**, 121 (2015).

[23] S. Chatterjee, B. Mohanty, R. Singh, *Phys. Rev. C* **92**, 024917 (2015).

[24] S. Borsányi *et al.*, *J. High Energy Phys.* **1009**, 073 (2010); Y. Aoki *et al.*, *J. High Energy Phys.* **0906**, 088 (2009); M. Cheng *et al.*, *Phys. Rev. D* **74**, 054507 (2006); J.B. Kogut, D.K. Sinclair, *Phys. Rev. D* **85**, 054505 (2012).